CIRRUS PROPERTIES AND CLOUD SCALE DYNAMICS FROM MM-WAVELENGTH

DOPPLER RADAR MOMENTS RETRIEVAL: TROPICAL

AND MID-LATITUDE CIRRUS COMPARISON

Min Deng* and Gerald G. Mace
Department of Meteorology, University of Utah, Salt Lake City, Utah, 84112, U. S. A

1. INTRODUCTION

Millimeter cloud radar (MMCR) observations collected by the Atmospheric Radiation Measurement (ARM) program provide a unique opportunity to study and compare the properties of tropical and middle latitude cirrus clouds. Doppler measurements provide a power spectrum as a function of the particle fall velocity, which is related to the particle size (Mitchell, 1996). Moreover, the second Doppler moment σ_d, or Doppler spectrum width, is a measurement of the spread of the signal in the Doppler velocity domain, and is attributed to the presence of particles with different terminal velocities and the turbulence within the radar sample volume.

In this paper, an innovative radar-only algorithm, using the first three moments of the Doppler spectrum to estimate the cloud microphysical properties and the mean air motion, is briefly introduced in section 2. The sensitivity and error analysis are shown section 3. In section 4, the algorithm validation is made with in situ measurements. Then the algorithm is applied to 1-year MMCR data collected by ARM at the Tropical Western Pacific Nauru (TWPC2) and the Southern Great Plain (SGP) sites. The seasonal variations of cirrus properties at these two sites are shown and compared. A strong temperature dependence of IWC is found. Comparing with available parameterizations of IWC of cirrus cloud in numerical models, a mass weighted particle fall velocity parameterization based on the radar retrieval dataset is proposed. With the retrieval results from the 35 GHz MMCR observations at the ARM SGP and TWP sites, the mass weighted particle fall velocity is parameterized as a function of IWC and temperature. The results are shown in section 5.

2. FORWARD MODEL DEVELOPMENT

According to Gossard (1994), and Babb (1999), the millimeter cloud radar (MMCR) Doppler spectrum is broadened by air turbulence through a convolution of the quiet air reflectivity spectrum with the air motions in the sample volume. In this study, a cloud property and air motion retrieval algorithm is developed using only MMCR moments (Deng and Mace, 2005).

Corresponding author's address: Min Deng, Department of Meteorology, University of Utah, Salt Lake City, Utah, E-Mail: mdeng@met.utah.edu.

2.1 *Quiet Air Doppler Spectrum and Radar Moments*

First, considering the quiet air radar volume, the water equivalent radar reflectivity factor Z_e is expressed as the integration of the radar reflectivity density function.

$$Z_e = \int_0^\infty a_z \times D^{6+b_z} N(D) dD = \int_0^\infty S(D) dD \quad (1)$$

where the parameters a_z and b_z are found through a power law fit (Mace 2002), and $N(D)$ is the particle size distribution. So the radar reflectivity density function is

$$S_z(D) = a_z \times D^{6+b_z} N(D) \cdot \quad (2)$$

Some researchers have suggested that the particle size versus number concentration spectra can be well represented by one or more exponential regimes. So here we consider a simple exponential particle size distribution (PSD) function, and then the quiet air spectrum density function is:

$$S_z(D) = a_z \times N_o \times \exp(-\lambda \times D) \times D^{6+b_z} \quad (3)$$

where the N_o is the drop concentration mode, λ is the exponential slope. However, the observed radar spectra are a function of Doppler velocity. Fortunately, the relationship between terminal velocities of particles in quiet air versus particle size has been studied (Heymsfield, 2000, Mitchell, 1996), and can be fitted by a power law function according to in situ measurements.

$$D(cm) = a_d \times V_f^{b_d}, \quad (4)$$

where the a_d and b_d are parameters of the power law function, and with

$$Z_e = \int S_z(D) dD = \int S(V_f) dV_f, \quad (5)$$

the transformed quiet air reflectivity spectral density function as a function of falling velocity is:

$$S(V_f) = N_0 \times a_z \times b_d \times a_d^{(7+b_z)} \times V_f^{(b_d \times (7+b_z)-1)} \times \exp(-\lambda \times a_d \times V_f^{b_d}) \quad (6)$$

Through equations (5) and (6), we can calculate the radar reflectivity through integration. The mean Doppler velocity (V_d) and Doppler spectrum width (σ_d) can also be integrated as described in Mace, et al. 2002.

2.2 *Convolution With Air Motion*

The real reflectivity spectrum $S(w_i)$ is composed by convolution of quiet air spectrum $S(V_f)$ with the probability density function PDF) $G(w_j)$ of turbulence:

$$S(w_i) = \int_{-\infty}^\infty G(w_j) \times S(V_f = (w_i - w_j)) \times dw_j \quad (7)$$

For convenience in the integrations, the air turbulence is represented by an exponential PDF given by:

$$G(w_j) = \frac{1}{2 \times W_\sigma} \times \exp(-\frac{|w_j - w_m|}{W_\sigma}) \qquad (8)$$

where W_m is the mean air velocity and W_σ represents the intensity of air turbulence. Gossard (1994) has demonstrated that this devolution technique is not very sensitive to the exact functional form chosen for the air turbulence spectrum.

With the convolution model, the observed reflectivity spectra at ith velocity bin is a function of N_0, λ, W_m, and W_σ. We can express the turbulence-convolved spectrum density function in terms of the mean air motion (W_m) as shown in equations (9) and (10), respectively:

$$S_{z1}(w_i) = \frac{1}{2 \times w_\sigma} \int_{-\infty}^{w_i} S_0 \times (w_i - w_j)^{b_d(7+b_z)-1} \times \exp(-a_d \lambda (w_i - w_j)^{b_d}) \times \exp(\frac{w_j - w_m}{w_\sigma}) dw_j, \qquad (w_i < w_m) \quad (9)$$

$$S_{z2}(w_i) = \frac{1}{2 \times w_\sigma} \{ \int_{-\infty}^{w_m} S_0 \times (w_i - w_j)^{b_d(7+b_z)-1} \times \exp(-a_d \lambda (w_i - w_j)^{b_d}) \times \exp(\frac{w_j - w_m}{w_\sigma}) dw_j +$$

$$\int_{w_m}^{w_i} S_0 \times (w_i - w_j)^{b_d(7+b_z)-1} \times \exp(-a_d \lambda (w_i - w_j)^{b_d}) \times \exp(\frac{w_m - w_i}{w_\sigma}) dw_j \} \qquad (w_i > w_m) \quad (10)$$

The net effect of convolution is to broaden and shift the original quiet air radar spectrum (figure not shown). From the simulated spectrum (Eqn. 9 and 10) we can calculate the first three Doppler moments through integration. However, the retrieval problem is ill conditioned with three measurements to solve four unknowns. In the current algorithm W_σ is not retrieved but considered as a parameter and estimated from radar reflectivity and Doppler spectrum width.

The estimation of W_σ is based on two empirical observations. First, the actual range of W_σ in cirrus tends to be narrow from ~0 to 30 cm/s as derived from in situ data (from the CRYSTAL-FACE and 2000 IOP measurements). Second, from the forward model sensitivity study we can shown that the particle spectrum width primarily contributes to W_σ. Moreover, for the interested range of particle size, the spectrum width is not very sensitive to W_σ (Figure not shown).

3. SENSITIVITY STUDY AND ERROR ANALYSIS

One of source of uncertainty in the retrieval arises from the exponential particle size distribution assumption. The procedure to estimate this sensitivity is to compute the radar moments from aircraft vertical velocity and particle spectra using numerical integration. Then from these radar moments the microphysical properties and air mean velocity are retrieved assuming an exponential PSD or modified Gamma PSD with α (the breadth of the PSD) equal to 3 or 5.

Several examples of particle size spectra and associated retrieved spectra are shown in Figure 1. In each panel, the triangle, asterisk, and diamond represent in situ observations, exponential PSD retrieval and gamma PSD retrieval with α equal to 5, respectively. The results illustrated in figure 1a favors the exponential PSD assumption even though the in situ PSD has somewhat smaller concentrations of large particles leading to an estimate of D_{mass} from the exponential assumption that is slightly larger than the in situ measurements. In Figure 1b, the concentration of small particles is smaller and the gamma PSD retrieval does better. The case in Figure 1c begins to show bimodality. Even though the assumed exponential PSD or gamma PSD has the same integrated radar moments, the retrieved particle size underestimates the ensemble mass weighted particle length by about 40% and 25%, respectively, because the single mode distribution functions overestimate the concentration of small particles. In Figure 1d, bimodality is even more significant so that the exponential PSD and gamma PSD retrieval underestimate the particle size by about 60% and 30%, respectively.

Based on 1800 5-second averages of aircraft measurements, about 85% could be retrieved with an exponential or Gamma PSD within reasonable retrieval error. This is consistent with the results in
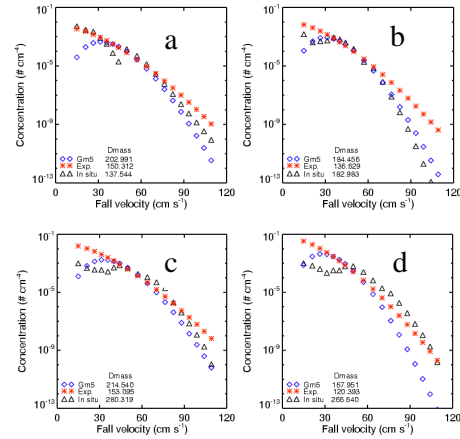
Figure 1. Examples of the in situ PSD in comparison to the retrieved exponential and gamma PSD with α equal to 5. The in situ PSD is plotted as a black triangle, the retrieved exponential PSD is plotted as a red asterisk, and the retrieved gamma PSD with α equal to 5 is plotted in blue diamond.

Mace et al. (2002) that single mode functions are able to capture the essential characteristics of these spectra within observational uncertainty for most cirrus.

The algorithm uncertainties due to the estimation of W_σ and empirical parameters are also examined. The sensitivity study shows that the error due to the power law parameters can be larger than that brought out by the estimation of W_σ. As a result, an accurate estimation of the empirical relationships is very important to the accuracy of this algorithm. Refer to Deng and Mace, 2005 for more detail.

4. ALGORITHM VALIDATAION

In situ data are very useful to validate our retrieval algorithm because of its direct sampling. The Citation data provide the PSD and high temporal resolution air (25 Hz) motions. Figure 2 is an over-plot of radar reflectivity and the flight track of the UND (University of North Dakota) Citation aircraft on Mar. 13, 2000. During the flight, the Citation sampled cirrus clouds from about 18.5 to 21.5 UTC. Particle spectra data files have been generated from the 2D-C and FSSP probe, which can detect particles ranging from 30 to approximately 1000 microns. The air motion data is obtained from 25 Hz data from the UND Citation. The comparison in Figure 3 shows good agreement between the retrieval and in situ measurement.
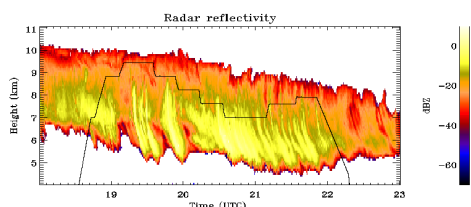
Figure 2. Radar reflectivity observation on March 13 2000 IOP at the ARM SGP. The aircraft flight track is over-plotted with black line.
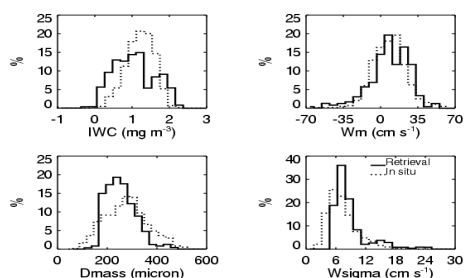
Figure 3. The histogram comparison between the retrieval and in situ data. The solid line is the retrieva.

5. ALGORITHM APPLICATIONS

The first application of this algorithm is to compare the retrieved cirrus properties between the mid-latitude and the tropics. The cirrus cloud macrophysical properties including cloud height and temperature are collected from the radar measurements and sounding data during the period July, 1999 – July, 2000. The corresponding microphysics and the cloud-ambient air mean velocity are retrieved using the current algorithm. The results are shown in Figure 4 with the black line for the TWPC2 and the orange line for the SGP. Considering the different sensitivities of the radars at these two sites, the results at the SGP site are also shown in terms of clouds with radar reflectivity larger than -40dBZ (blue line), which is roughly the minimum signal at the TWPC2. The increased minimum reflectivity threshold at SGP excludes cirrus about 10% of the cases which tend to be composed of smaller particles and ice masses at relatively colder temperature. The figure shows that in general, the tropical cirrus clouds are higher with larger ice particles and greater mass, which correspond to larger mass weighted fall velocities. Moreover, the distribution of the cloud ambient air vertical velocities at the SGP is almost symmetrical between upward and downward motion with the mean at about -6cm/s. While the cloud-ambient air vertical velocities at the TWPC2 suggests upward motion and average about -24 cm/s.

The seasonal variation of cirrus observed at SGP and TWPC2 are shown in figure 5 and 6. For the SGP site, cirrus in the summer have larger IWC, concentration and size than those in the winter. Moreover, in the winter, the distributions of cloud properties are narrower compared to summer. For the cirrus observed at TWPC2, the seasonal variation is small as expected.

The IWC distribution is important to calculate radiative transfer of ice clouds because the cloud optical depths are primarily dependent on it (Platt and Harshvardhan, 1988). With a conceptual model of idealized deposition of a lifted moisture layer and crystal settling, Heymsfield and Donner 1990 proposed a scheme for parameterizing ice-cloud water content in general circulation models with temperature and the large scale vertical velocity. There are also several papers (Illingworth et al, 1999, Heymsfield, 2003, Mitchell, 1996) relating the IWC with temperature or the mass weighted fall velocity (Vf_{mass}), another important parameter in GCMs. The model studies have shown that the ice particle sedimentation velocity has an impact on the precipitation, cloudiness and radiative forcing (Klein and Jakob, 1999). For some GCMs (ECMWF; UKMO; Geophysical Fluid Dynamics Laboratory (GFDL; Donner et al, 1999)), the ice precipitation is allowed to fall between levels and is retained from one time step to the next with a rate that is determined by the IWC using the characteristics of the particle size distribution. In this section, we specify the Vf_{mass} in terms of temperature and IWC using the above retrieved dataset from the ARM TWPC2 and

SGP sites. This parameterization may be helpful for climate models since it bounds the fall speed of upper tropospheric ice using observations.

By definition, the Vf_{mass} can be expressed as a function of N_o and λ. Connected with IWC, it can be written as:

$$\log(Vf_{mass}) = a\log(N_o) + b\log(IWC) \quad (11)$$

As some papers (Houze et al. 1979, Ryan, 1996) have suggested that the intercept of the particle size distribution (N_o) may be related to the exponential of temperature, thus, Equation 11 can also be written as:

$$\log(Vf_{mass}) = a'T + b\log(IWC) \quad (12)$$

The retrieved results at the ARM SGP and TWPC2 are plotted in 2d histogram in terms of IWC and temperature in Figure 7. The top panel shows the cirrus cloud frequency distribution in IWC and temperature. These frequency distributions show that the IWC depends strongly on temperature: the warmer the cloud volume, the larger the IWC tends to be (with substantial variability about the mean). The middle panel shows the grid mean mass weighted fall velocity of cirrus within the corresponding temperature and IWC bins. It shows that the mass weighted particle fall velocity generally increases with IWC. However, not only the intercept but also the slope are functions of temperature. With this interpretation, b in Equation 12 should be a function of temperature as well. According to the above physical derivation and actual observations, the relationship between the Vf_{mass}, IWC, and T can be formulated as:

$$\log(Vf_{mass}) = aT\log(IWC) + b\log(IWC) + cT + d$$
$$(13)$$

The units for Vf_{mass}, IWC, and T, are cm s^{-1}, mg m^{-3}, and K, respectively. Comparison between these two sites shows that the Vf_{mass} at both sites has a similar distribution as a function of IWC and T even though absolute values are different. In addition, cirrus clouds at the SGP site are never observed by the radar to be colder than 200 K. However, this may be overstated because the MMCR fails to detect cold thin cirrus (Wang, 2002, Comstock, 2002). The fitted results are shown in the bottom panels in figure 7. The correlation coefficient between the fitted results and retrieval is above 0.8 for both sites. The fitted parameters for SGP and TWPC2 are listed in table 1. However, the results should be considered preliminary until more data are used for the analysis.

6. SUMMARY

The first three moments of the millimeter wavelength radar Doppler spectrum provide valuable information regarding both cloud properties and air motions. An algorithm using the Doppler radar moments is developed to retrieve cirrus microphysical properties and the air mean vertical motion and their errors. This technique utilizes a statement that the observed Doppler spectrum is a convolution between a spectrum of air motions and a radar reflectivity spectrum from cloud particles that exist in air that has

no mean motion or turbulence. The set of equations describing the Doppler spectrum
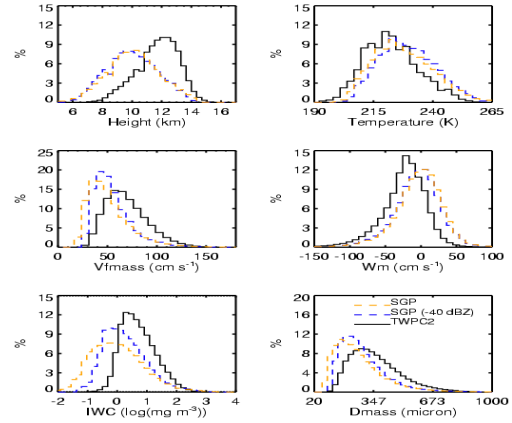
Figure 4. The comparison of cirrus cloud properties and cloud-ambient air mean velocity between the ARM SGP (yellow line) and TWPC2 (black line) sites. Consider the different sensitivity of radars at these two sites, the results at the SGP site is also shown in terms of clouds with radar reflectivity larger than -40dBZ (blue line), which is the minimum signal at the TWPC2.
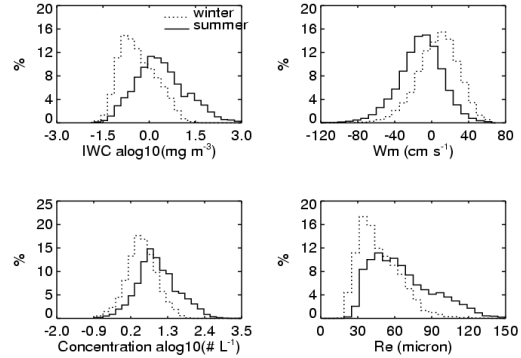
Figure 5. The cirrus cloud properties and cloud ambient air mean velocity at ARM SGP site.
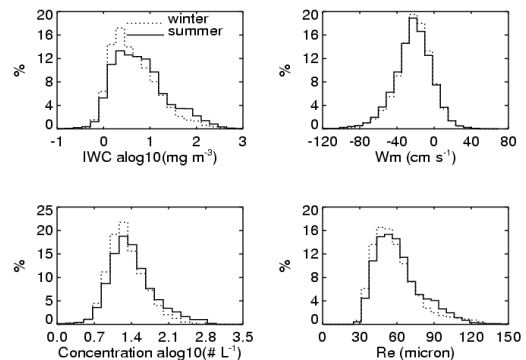
Figure 6. The same as figure 6 except at ARM TWPC2 site.
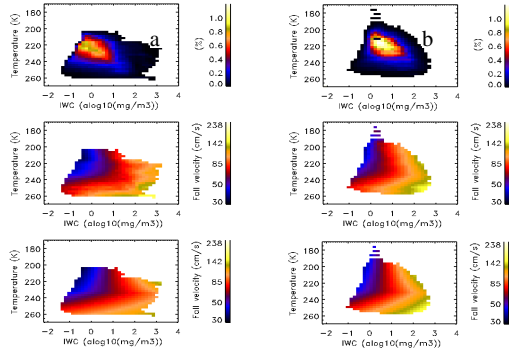
Figure 7. The mass weighted fall velocity (Vf$_{mass}$) in terms of temperature and IWC at the ARM SGP (column a) and TWPC2 (column b). The top two figures show the frequency distribution of cirrus in terms of temperature and IWC. The middle figures show the mean Vf$_{mass}$ of cirrus cloud in the bin. The bottom two figures show the fitted Vf$_{mass}$ as a function of temperature and IWC using Equ. 13.

Table 1. The coefficients for the parameterization of mass weighted fall velocity as a function of temperature and IWC using Equ.13 for cirrus observed at the ARM SGP and TWPC2 sites shown in Figures 7. The numbers below the sites designations are the total number of bins of data used at each location. T$_c$ is the critical temperature. See Deng and Mace, 2005 for more detail.

site	T$_c$	a	b	c	d
SGP	T<235.0	-0.0235	-4.32	-0.190	- 11.18
(576864)	T>235.0	-0.00163	0.0158	0.0055	2.17
TWPC2	T<232.5	0.1524	11.296	-0.351	-25.73
(789302)	T>232.5	-0.00180	0.0471	0.051	2.312

moments in terms of the cirrus particle size distribution and air motion distribution function are inverted using optimal estimation theory to derive the particle size distribution, the mean vertical velocity of the air in the sample volume, and the objectively derived retrieval error. The error analysis shows that the retrieval algorithm results are very sensitive to the power law relationships describing the ice particle mass and the terminal velocity in terms of the particle maximum length. Algorithm validation with in situ data demonstrates that the algorithm can determine the cloud microphysical properties and air mean velocity with reasonable errors: 50% for IWC, 30% for the particle size, and ±15cm/s for the air mean vertical velocity in the radar sample volume.

The algorithm is applied to MMCR data collected at Atmospheric Radiation Measurement sites from the tropics and middle latitudes. The comparison between these two sites shows that the cirrus in the tropics are generally colder and higher with larger ice particles and mass, which correspond to larger mass weighted fall velocities. Moreover, the tropical cirrus tend to be more likely observed within ascending air parcels compared to mid-latitude cirrus clouds.

A parameterization of cirrus mass weighted fall velocity as a function of temperature and IWC is proposed.

7. REFERENCE

Babb, D. M., 1999, Retrieval of could microphysical parameters from 94-GHz radar Doppler power spectra. *J. Atmos. Ocean. Tech.*, **16**, 489-503.
Deng, M and G.G Mace, 2005: Cirrus microphysical properties and air motion stataistic Using cloud radar Dopper Moments: Part I – algorithm Description. Submitted to JAM
Donner, L. J. C. J. Seman, R. S. Hemler, 1999: Three-dimensional cloud system modeling of GATE convection. *J. Atmos. Sci.*, **56**, 1885-1912.
Gossard, E.E., 1994, Measurement of cloud droplet size spectra by Doppler radar. *J. Atmos. Ocean. Tech.*, **11**, 3, 712-726.
Hemsfield A. J. and L. J. Donner, 1990: A scheme for paramterizing ice-cloud water contence in general circulation models. J. Atmos. Sci., **47**, 1865-1877.
Heymsfield A. J., 2003: Properties of tropical and midlatitude ice cloud particle ensembles. Part II: Applications for mesoscale and climate models. *J. Atmos. Sci.* **60**, 2592-2611.
Heymsfield, A. J., and J. Iaquinta, 2000, Cirrus crystal terminal velocities, J. Atmos. Sci., **34**, 916-938.
Houze, R. A. Jr. S. G. Geotis, F. D Marks, 1979: Stratiform precipitation in region of convection: A meteorological paradox. *Bull. Amer. Meteor. Soc.* **78**, 2178- 2196.
Klein S. A. and C. Jakob, 1999: Validation and sensitivities of frontal clouds simulated by the ECMWF model. *Mon. Wea. Rev.* **127**, 2514-2531.
Liu, C, A. J. Illingworth, 2000, Toward more accurate retrievals of ice water content from radar measurements of clouds. *J. Appl. Metero.*, **39**, 1130-1146.
Mace G. G., T. P. Ackerman, P. Minnis, D. F. Young, 1998: Cirrus layer microphysical properties derived from surface-based millimeter radar and infrared interferometer data. *J. Geophys. Res.*, **103**, 23207-23216.
Mace, G, G, 2002: On retrieving the microphysical properties of cirrus clouds using the moments of the millimeter-wavelength Doppler spectrum. *J. Geophys. Res.* **107**, 4815-4831
Mitchell, D., 1996, Use of Mass- and area-dimensional power laws for determining precipitation particle terminal velocities. *J Atmos. Sci.* **53**, 1710-1723.
Platt, C. and M. R. Harshvardhan, 1988: Temperature dependence of cirrus extinction: Implications for climate feedback, *J. Geophys. Res.*, **98**, 11051-11058.